

# Processing of tissue sensing adaptive radar data - an analogue for georadar

Adrian Smith\*, Jérémie Bourqui, Youhong (Kay) Liu, Elise Fear, Robert Ferguson

adrsmith@ucalgary.ca

## Abstract

Frequency domain georadar data have several advantages over time domain data but are much more cumbersome to acquire. A medical imaging technique developed in the Department of Electrical Engineering at the University of Calgary known as "tissue sensing adaptive radar" (TSAR) makes use of monostatic radar data acquired in the frequency domain. Simulated data were generated and processed using a workflow that has been previously developed and implemented successfully on georadar data. We discover that the simulated TSAR data are mixed phase, violating the minimum-phase assumptions of deconvolution. We show through synthetic examples that deconvolution of these data does not recover reflectivity accurately. Although nonstationary Gabor deconvolution has been shown to be effective when applied to georadar data, our work with the TSAR data shows that we must take care to ensure that radar data be minimum phase during deconvolution, especially with data acquired in the frequency domain.

## Radar Reflection Method

Many disciplines including georadar and medical imaging use the radar reflection method. It is analogous to seismic reflection in several ways, including the formulation of the reflection coefficient ( $R$ ) for normal incidence:

$$R = \frac{\sqrt{\epsilon_{r1}} - \sqrt{\epsilon_{r2}}}{\sqrt{\epsilon_{r1}} + \sqrt{\epsilon_{r2}}}, \quad (1)$$

where  $\epsilon_{r1}$  and  $\epsilon_{r2}$  are the relative electric permittivities of the incident and transmission media respectively. Assuming a low-loss geological environment, the relative electric permittivity is related to the velocity ( $v$ ) of electromagnetic radiation in a medium by:

$$v = \frac{c}{\sqrt{\epsilon_r}}, \quad (2)$$

where  $c$  is the speed of light in a vacuum ( $c \approx 0.3$  m/ns).

## Tissue Sensing Adaptive Radar (TSAR)

- ▶ Prototype diagnostic breast imaging method, designed to complement other breast cancer detection techniques.
- ▶ Uses monostatic frequency domain radar acquisition. Reflections of interest arise from differences in  $\epsilon_r$  between healthy and diseased tissue.

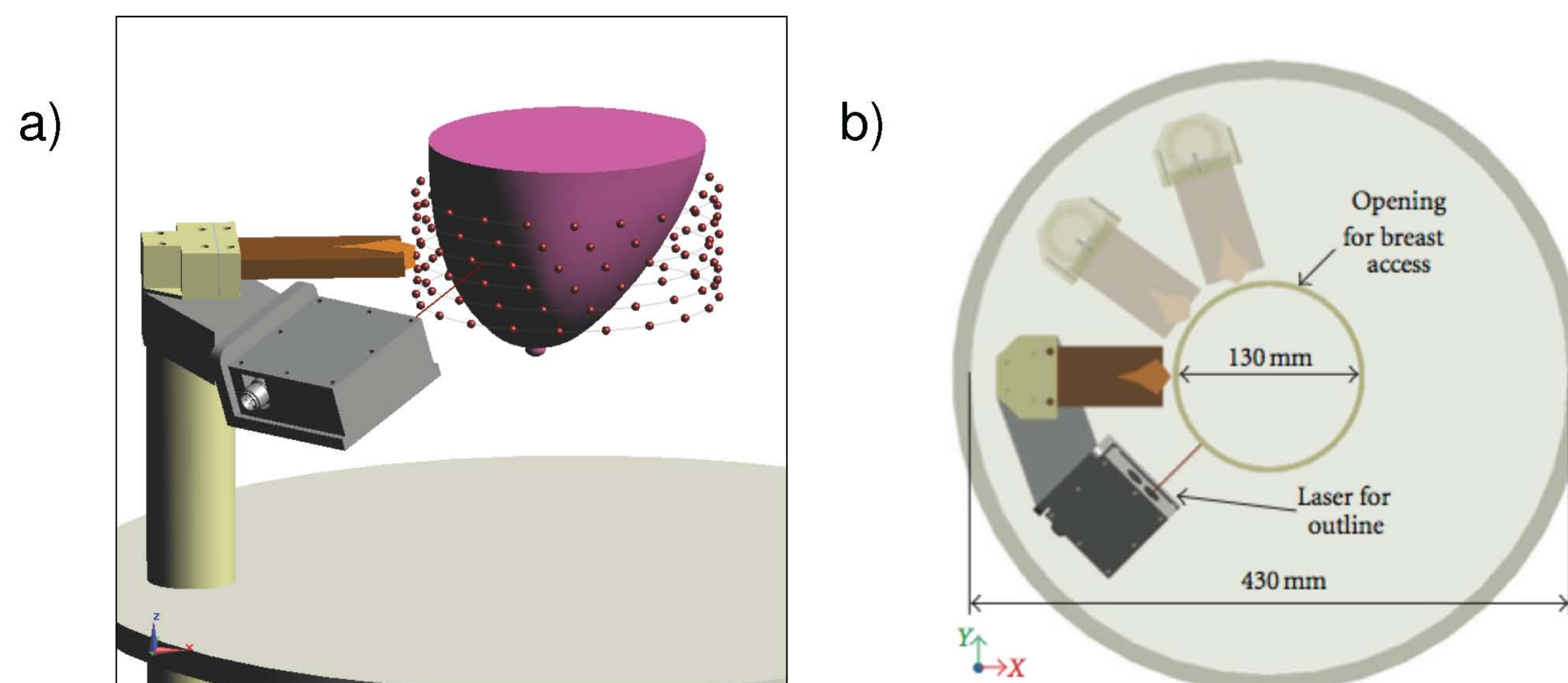


Figure 1: 3D illustration of the prototype TSAR system. View of the scan pattern used for measurement a). Each small red sphere corresponds to an antenna location. A plan view of the device is shown in b). The laser is used to determine the distance from the antenna aperture to the irregular surface of the skin on the breast.

## TSAR Simulation

- ▶ TSAR-like data were simulated using software developed by the Department of Electrical Engineering at the University of Calgary.
- ▶ Balanced Antipodal Vivaldi Antenna with Director (BAVA-D) used.
- ▶ An inclusion of relatively higher  $\epsilon_r$  was imbedded in simulation space as a future imaging target (Figure 2).

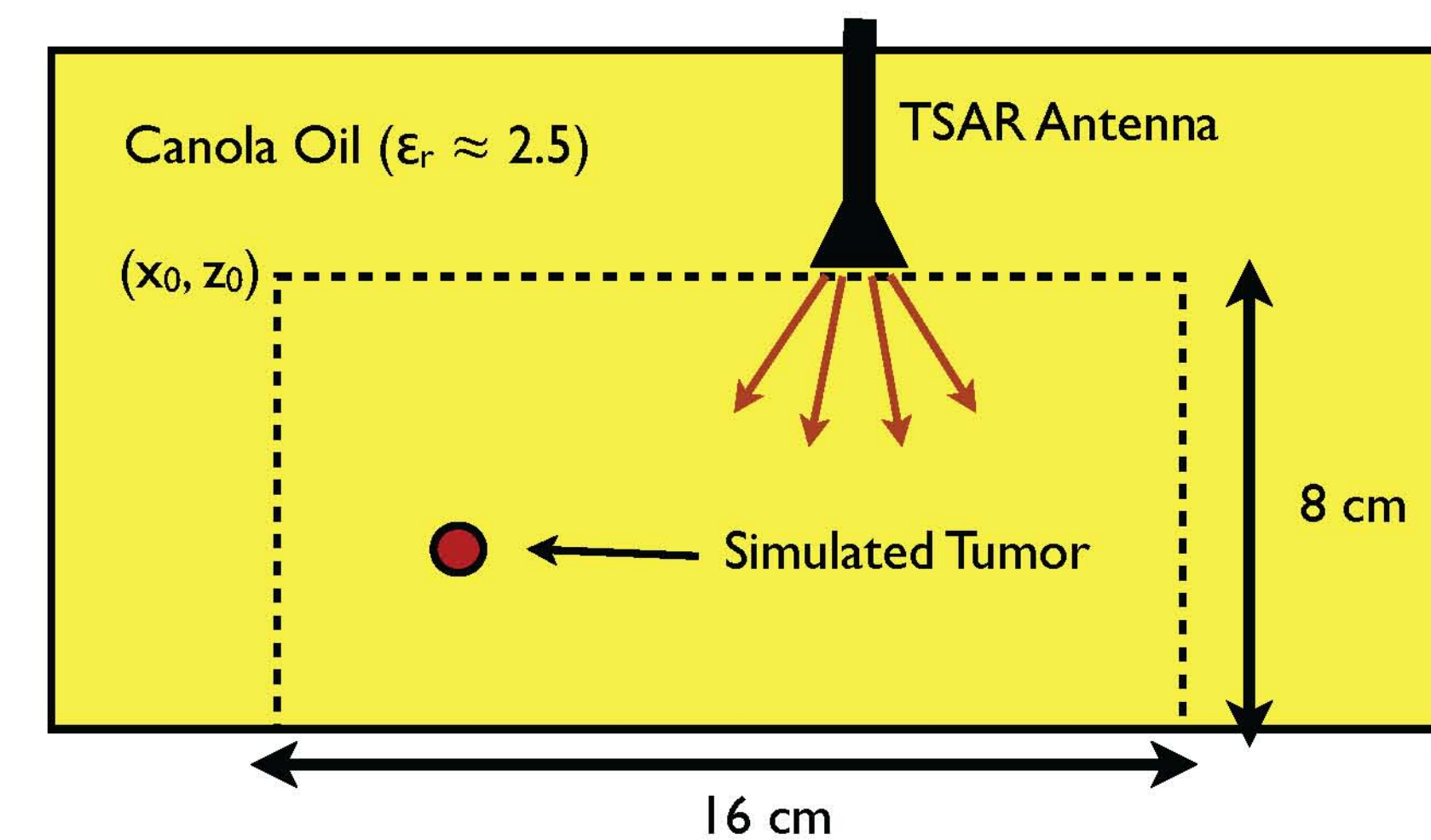


Figure 2: Schematic of TSAR simulation space. See table below for acquisition parameters.

Parameter	Value
Sensor Spacing	0.001 m
Number of Locations	101
Frequency Range	0 - 14.99 GHz
Frequency Step	10 MHz

The source TSAR pulse has a form of:

$$v(t) = V_0 \cdot (t - t_0) \cdot e^{-\frac{(t-t_0)^2}{\tau^2}}, \quad (3)$$

where  $V_0$  is used to adjust the amplitude,  $\tau = 62.5$  ps and  $t_0 = 4\tau$ .

## Pre-Processing

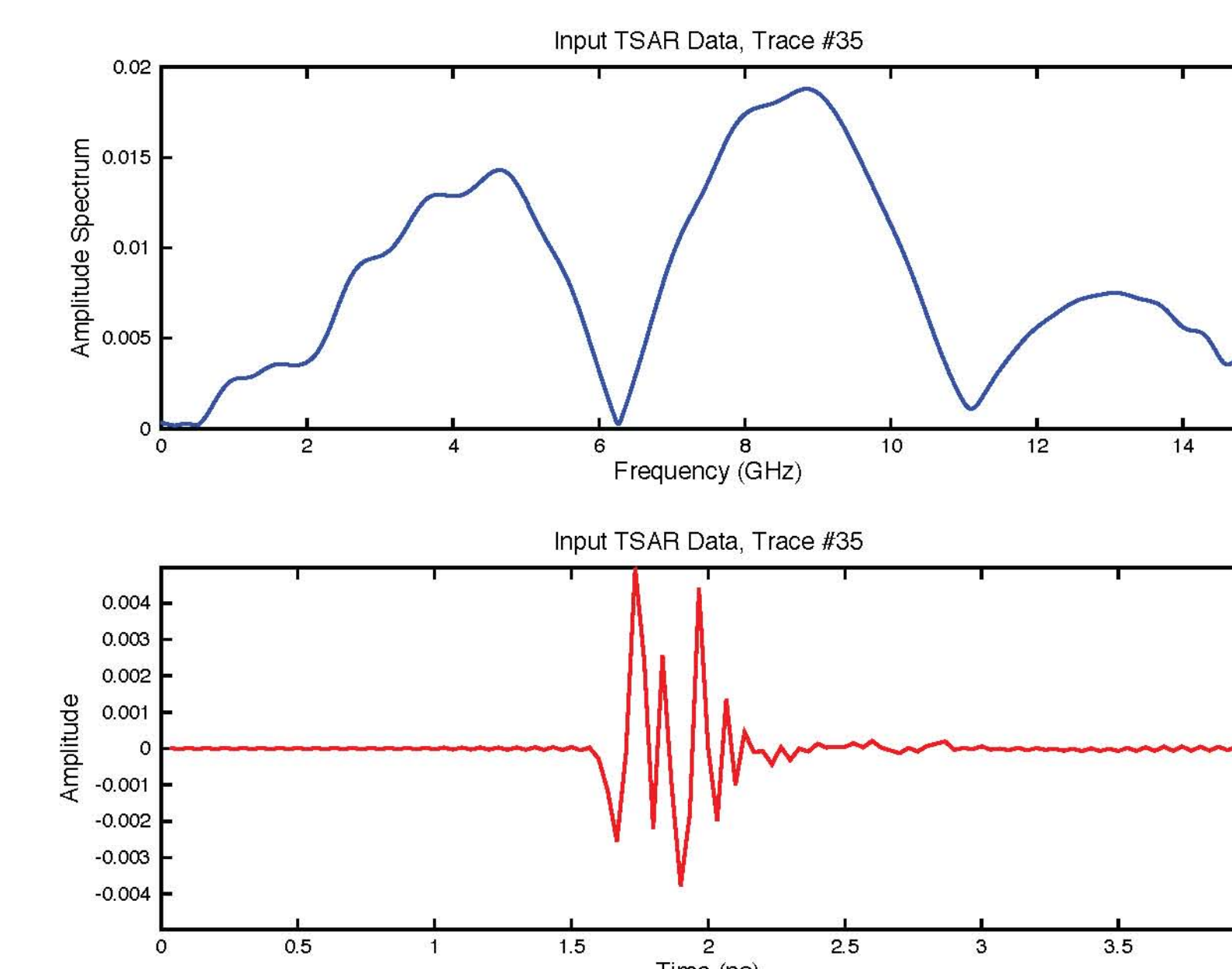


Figure 3: Simulated TSAR data from a single trace. Upper image represents raw frequency domain data, lower image is a time domain reconstruction using *bltfft* from the CREWES MATLAB toolbox.

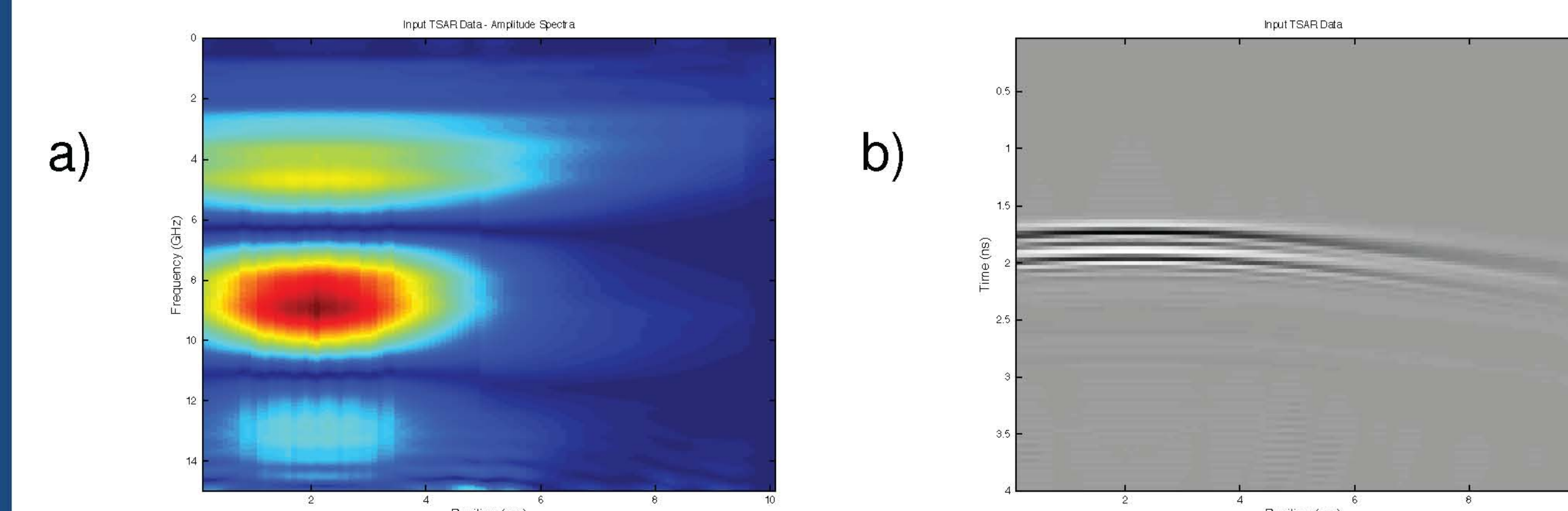


Figure 4: Simulated TSAR data for the entire record. Raw frequency domain data a), and time domain reconstruction using *bltfft* from the CREWES MATLAB toolbox.

## Pre-Processing Continued

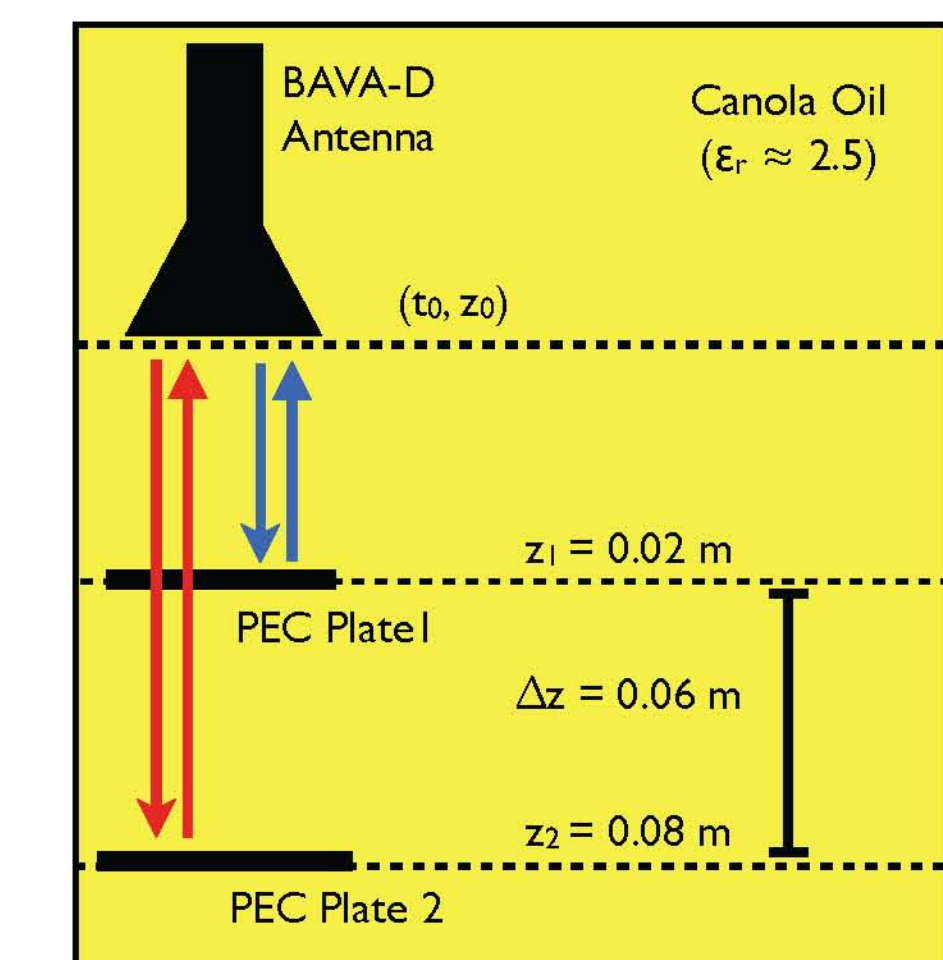


Figure 5: Schematic illustrating determination of  $z_0 = 0$  m location in time. Two perfectly electrically conducting (PEC) plates are individually placed in the simulation at known  $z$  locations, and the two-way-traveltimes (TWT) from each reflection recorded. From this, the velocity of the medium was estimated as well as the time shift needed to reposition to the data to the proper  $z_0 = 0$  m location.

## Wavelet Phase Decon Test

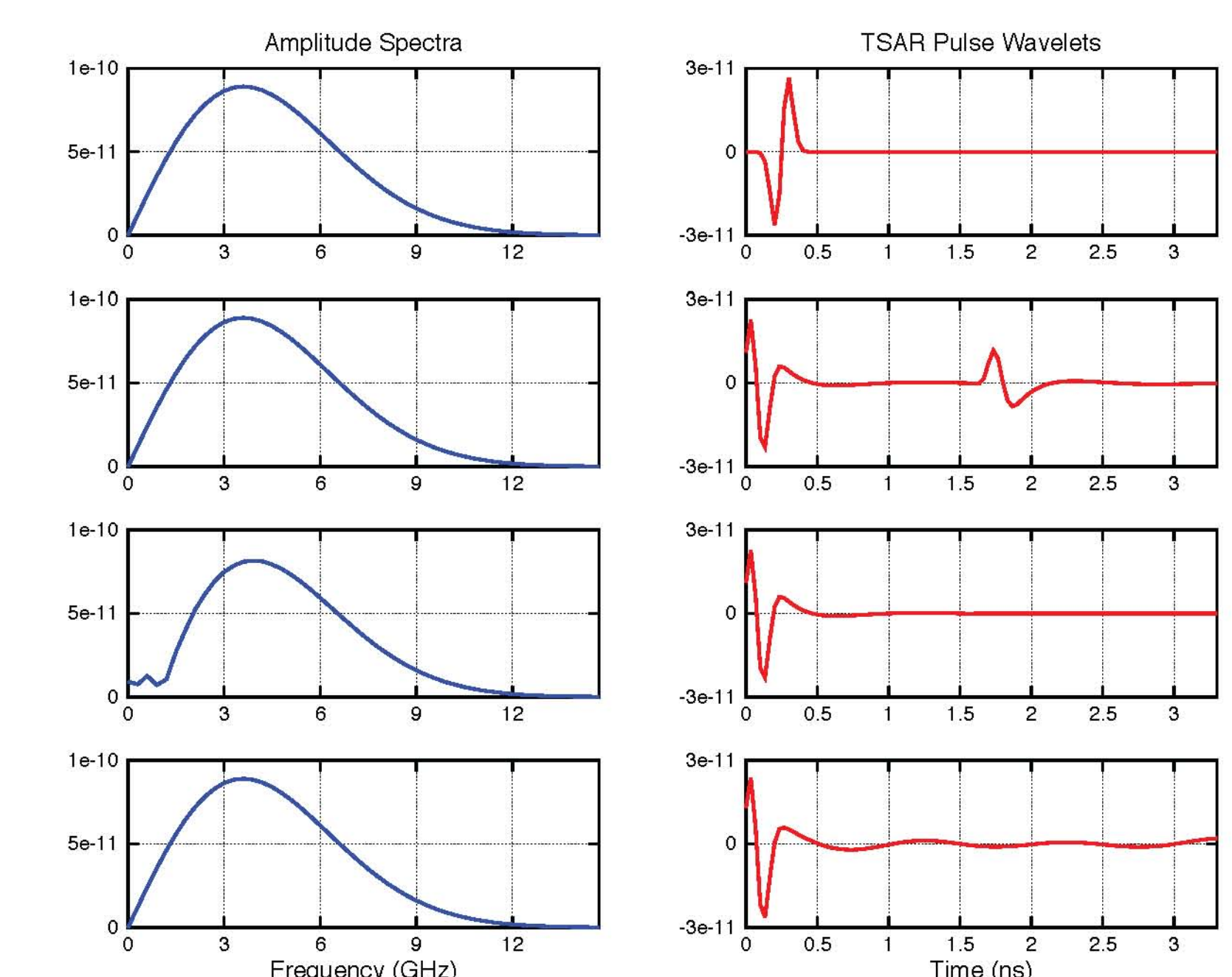


Figure 6: Minimum phase equivalent wavelet construction. Top row is input analytic TSAR pulse and spectrum. Second row is minimum phase reconstruction using the *rceps* function in MATLAB. Third row is minimum phase reconstruction after zeroing the second half of the signal in the time domain. Bottom row is wavelet constructed with phase spectrum from row 3 and amplitude spectrum from the top row.

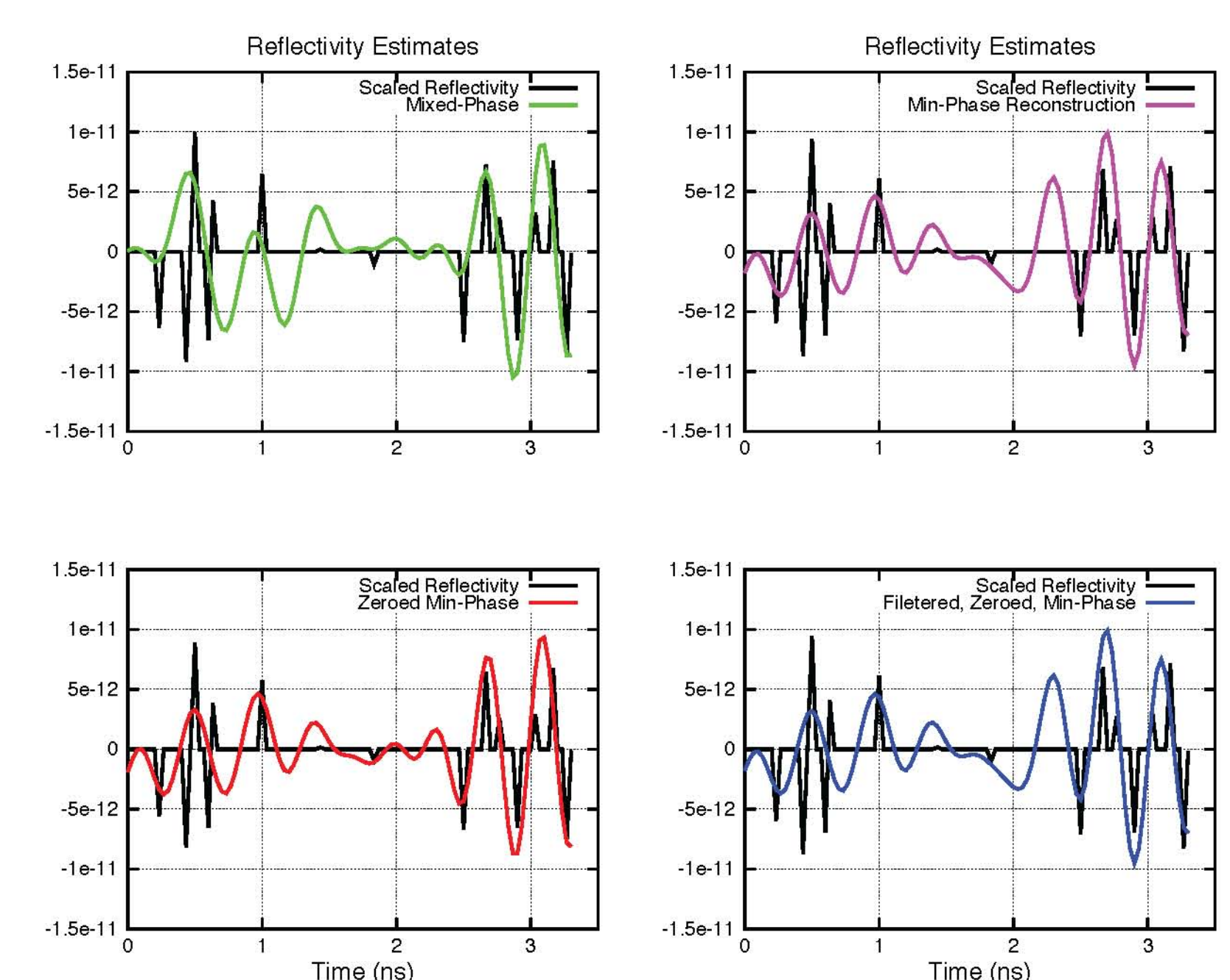


Figure 7: Recovered reflectivities from synthetics generated with four wavelets from Figure 6 using *gabordecon* from the CREWES MATLAB toolbox. Note the relatively poorer performance with the mixed-phase wavelet, especially on the cluster of reflectivity at 0.5 ns.

## Further Work

- ▶ Successfully perform nonstationary Gabor deconvolution and image the inclusions in the TSAR simulation.
- ▶ Ensure that other radar data is filtered to minimum phase before deconvolution to avoid erroneous results.